Highly Robust Multilamellar Lipid Vesicles Generated through Intervesicular Self-assembly Mediated by Hydrolyzed Collagen Peptides

Bon Il Koo,[a,1] Rafia Tasnim Rahman,[a,1] Jihui Jang,[b] Dong Jae Lee,[a] Jun Bae Lee,[b,*] and Yoon Sung Nam[a,*]

[a] Department of Materials Science and Engineering, Korea Advanced Institute of Science and Technology, 291 Daehak-ro Daejeon 34141, Republic of Korea
[b] Innovation Lab, Cosmax Research & Innovation Center, 662 Sampyong-dong, Bundang-gu, Seongnam, Gyeonggi-do, 13486, Republic of Korea

[*] Corresponding authors at: Innovation Lab, Cosmax Research & Innovation Center, 662 Sampyong-dong, Bundang-gu, Seongnam, Gyeonggi-do, 13486, Republic of Korea (J.B. Lee); Department of Materials Science and Engineering, Korea Advanced Institute of Science and Technology, 291 Daehak-ro Daejeon 34141, Republic of Korea (Y.S. Nam)
E-mail addresses: yoonsung@kaist.ac.kr (Y.S.N.) and jblee@cosmax.com (J.B.L.),
[1] These authors have equal contributions.

Abstract

Despite the advantages of lipid vesicles for drug and gene delivery, structural instability limits their practical applications and requires strictly regulated conditions for transport and storage. Chemical crosslinking and *in situ* polymerization have been suggested to increase the membrane rigidity and dispersion stability of lipid vesicles. However, such chemically modified lipids sacrifice the dynamic nature of lipid vesicles and obfuscate their *in vivo* metabolic fates. Here we present highly robust multilamellar lipid vesicles through the self-assembly of pre-formed, cationic large unilamellar vesicles (LUVs) with hydrolyzed collagen peptides (HCPs). The cationic LUVs undergo vesicle-to-vesicle attachment and structural reorganization through polyionic complexation with HCPs, resulting in the formation of multilamellar collagen-lipid vesicles (MCLVs). The resulting MCLVs exhibit excellent structural stability against variations in pH and ionic strength and the addition of surfactants. Particularly, the MCLVs maintain their structural stability against repeated freeze-thaw stresses, proving the excellent stabilization effect of HCPs on lipid lamellar structures. This work provides a practically attractive technique for the simple and quick fabrication of structurally robust lipid nanovesicles without covalent crosslinkers, organic solvents, and specialized instruments.

Keywords: multilamellar lipid vesicles; hydrolyzed collagen peptide; self-assembly; colloidal stability; freeze-thaw cycles

1. Introduction

Lipid nanovesicles have been extensively studied and developed for drug and gene delivery because of their biodegradability, excellent biocompatibility, and efficient intracellular delivery [1,2]. In the lipid film hydration and membrane extrusion method, hydrophobic drugs are dissolved with lipids in an organic solvent, and hydrophilic molecules are entrapped within vesicles when a dried lipid film is hydrated in an aqueous solution [3]. Sonication is applied to the hydrated lipid film to generate vesicular colloids, and membrane extrusion is used to generate large unilamellar vesicles (LUVs). High-pressure homogenization, also called microfluidization, has been also widely used for the large-scale production of lipid-based nanoparticles encapsulating various active molecules [4]. More recently, microfluidic technologies have been employed to prepare lipid nanoparticles with precise control over physical properties [5].

Although various fabrication techniques have been developed to produce lipid-based nanoparticles, their practical applications are still limited by intrinsic structural instability. As lipid molecules are self-assembled into vesicular structures via a delicate hydrophilic-hydrophobic balance, external physical and chemical stresses can induce the reversible dissociation of vesicles back to individual molecules or their reorganization to other structures. Such dynamic properties are unique features of lipid nanovesicles, which can be particularly advantageous as a nanocarrier for tissue penetration and intracellular burst release of active ingredients. However, the structural instability of lipid nanovesicles causes the leakage of active ingredients in the formulation during transport and storage, alters the release behavior *in vivo*, and induces aggregation and even precipitation. All of these undesirable structural changes can affect the *in vivo* efficacy of lipid-based formulations.

Several approaches have been investigated to increase the structural stability of lipid nanovesicles (**Fig. 1**). The *in situ* crosslinking and polymerization of pre-formed lipid vesicles are the most widely used techniques. Polymerizable lipids are used to make covalent linkages among the lipid molecules that are self-assembled to vesicular structures [6-8]. It is conceptually simple, but failure in the precise control of bilayer rigidity can cause significant membrane leakage. Similarly, small hydrophobic monomers can be incorporated into the non-polar region of the bilayer for in situ polymerization, which produces lipid-polymer hybrid vesicles [9]. On-surface grafting of multivalent polyelectrolytes to the exposed hydrophilic head groups of pre-formed lipid vesicles was also used to increase the mechanical strength of lipid bilayers [10]. Also, polymers were covalently bonded to the polar head of phospholipids to coat the surface of the lipid vesicles [11]. Multilamellar lipid vesicles were also fabricated using covalent crosslinkers, called interbilayer-crosslinked multilamellar vesicles (ICMVs) or multilamellar vaccine particles (MVPs), to increase the structural stability of lipid vesicles, which enhanced the loading efficiency of protein antigens and their delivery efficiency [12-14]. However, chemically reactive lipids can cause undesirable chemical modifications of the encapsulated ingredients, and the biological fates of covalent crosslinkers need to be extensively investigated to prove their long-term safety for clinical uses.

As an alternative to chemical modification, polyelectrolytes were deposited on the surface of liposomes in a single or layer-by-layer form by electrostatic attraction for the stabilization of lipid vesicles [15]. The hybrid vesicles coated with hydrophobic molecule-conjugated polymers also improved long-term stable circulation [16,17]. Recently, we reported

that some oppositely charged globular proteins can induce the structural changes of pre-formed charged lipid nanovesicles into multilamellar structures through polyionic interaction under certain conditions [18,19]. Our approach is similar to nucleic acid-lipid ionic complexation, where negatively charged nucleic acids are intercalated into the interstitial space of cationic lipid vesicles to generate closely packed arrays through spontaneous phase conversion [20-22]. However, protein-lipid complexation is technically more challenging as the precise control of the intermolecular interaction between proteins and the lipid membranes of nanovesicles is complicated because of the low and heterogeneous surface charge density of proteins. Accordingly, the approach has been applied only to a few specific proteins, such as M13 bacteriophage, actin filaments, and polyglutamic acid [23-25].

In this work, we suggest hydrolyzed collagen peptide (HCP) as a non-covalent crosslinker for lipid LUVs to induce their self-assembly into multilamellar collagen-lipid vesicles (MCLVs). HCP is a short peptide with a molecular weight of 3 – 6 kDa obtained by the acid/alkaline treatment and enzymatic hydrolysis of collagen [26]. HCP has received increasing attention for its pharmaceutical and biomedical applications due to its excellent biocompatibility and biodegradability. HCP is highly soluble in water and negatively charged at a neutral pH as its isoelectric point (pI) is in the range of 3.68 to 5.7, making it a good candidate for the layer-by-layer self-assembly of cationic LUVs. 1,2-Dioleoyl-3-trimethylammonium-propane (DOTAP) was used to produce cationic LUVs as it has been widely used as a transfection agent for nucleic acids and a component of EndoTAG® in a clinical trial [27]. Additionally, N-(9Z-octadecenoyl)phytosphingosine (ceramide NP or CNP) was introduced to enhance the robustness of the lipid vesicles. CNP is a major lipid component of the multilamellar stratum corneum in the skin and plays a role in strengthening the structure of lipid membranes [28,29]. Therefore, it was anticipated that CNP can contribute to the stabilization of lipid vesicles. The morphological changes, structural properties, and dispersion stability of the prepared MCLVs were investigated using cryogenic transmission electron microscopy (cryo-TEM), small-angle X-ray scattering (SAXS), fluorescence resonance energy transfer (FRET), and dynamic light scattering (DLS). This work emphasizes the structural stability of the resulting MCLVs under various conditions, including repeated exposure to freeze-thaw stress.

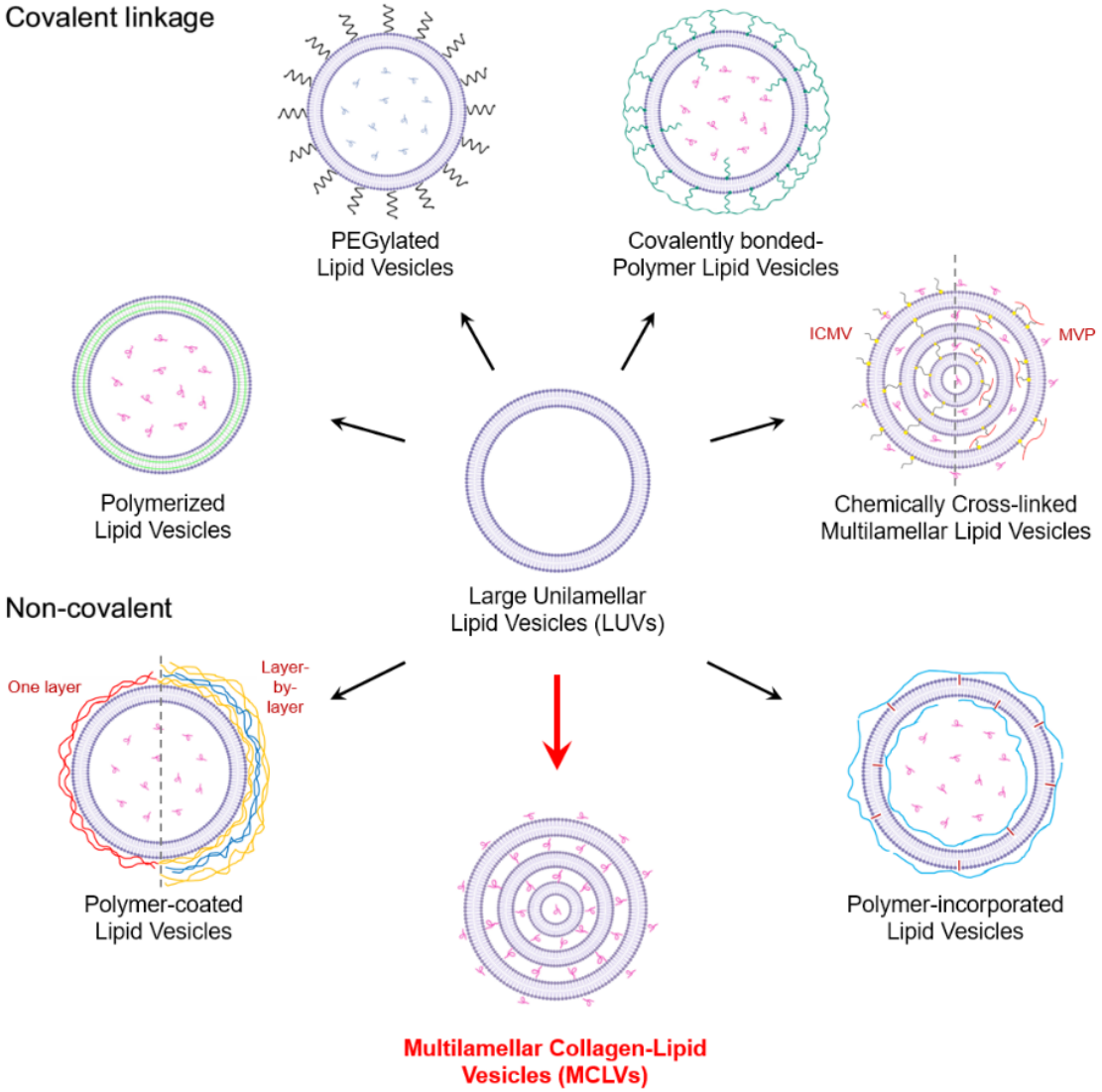

Fig. 1. Various lipid nanovesicles and their stabilization techniques. LUVs, polymerized lipid vesicles, PEGylated lipid vesicles, covalently bonded-polymer lipid vesicles, polymer-coated lipid vesicles, polymer-incorporated lipid vesicles, multilamellar vesicles with chemical crosslinkers, and multilamellar vesicles with non-covalent intercalators.

2. Experimental Section

2.1. Materials

HCP with a nominal molecular weight of 2.0 ± 0.5 kDa was purchased from Italgelatine SpA (Santa Vittoria d'Alba, Italy). DOTAP and CNP (DS-Ceramide Y3O, CNP ≥ 95 %) were obtained from Avanti Polar Lipid Inc. (Alabaster, AL, USA) and Solus Advanced Materials (Iksan-si, Jeollabuk-do, Republic of Korea), respectively. Chloroform was purchased from Junsei Chemical Co., Ltd. (Tokyo, Japan). Sodium chloride was obtained from Sigma-Aldrich (St. Louis, MO, USA). *N*-(Fluorescein-5-thiocarbamoyl)-1,2-dihexadecanoyl-*sn*-glycero-3-phosphoethanolamine, triethylammonium salt (fluorescein-DHPE) and *N*-

(tetramethylrhodamine-6-thiocarbamoyl)-1,2-dihexadecanoyl-*sn*-glycero-3-phosphoethanolamine (TRITC-DHPE) were bought from Invitrogen (Waltham, MA, USA) and AAT Bioquest Inc. (Mercury Drive, Sunnyvale, CA, USA), respectively.

2.2. Characterization of HCP

Matrix-assisted laser desorption ionization time-of-flight (MALDI-TOF) mass spectrometry was used to determine the molar mass of HCP. α-Cyano-4-hydroxycinnamic acid (CHCA) was used as a matrix and dissolved to saturation in a 1:1 mixture of deionized water and ethanol. HCP was dissolved in deionized water, and then the HCP solution was mixed with the prepared matrix solution and dried in air for 3 min. MALDI-TOF analysis was performed using Bruker autoflex III (Bruker Daltonics, Billerica, MA, USA). Circular dichroism (CD) analysis was carried out using a Jasco-815 CD spectropolarimeter (Jasco-815, Jasco. Inc., Tokyo, Japan) in the range of 185 – 260 nm. The CD profiles of HCPs were collected using a 0.2 mm path-length cell in deionized water. The composition of secondary structures was calculated by SpectraManager (Jasco. Inc., Tokyo, Japan).

2.3. Preparation of LUVs

The dissolved DOTAP in chloroform was dried with nitrogen gas to form a lipid thin film. The residual chloroform was eliminated by drying in a vacuum oven for 24 h. The dried lipid thin film was vigorously vortexed with deionized water at 37 ˚C for 2 h. The size of lipid vesicles was decreased using a mini extruder kit (Avanti Polar Lipid Inc., Alabaster, AL, USA) with a 0.1 μm polycarbonate membrane. The hydrodynamic size and zeta potential of the particles were determined using dynamic light scattering (DLS, ELSZ-1000, Otsuka Electronics, Osaka, Japan). For FRET analysis, fluorescence-labeled LUVs were produced using DOTAP, fluorescein-DHPE, and TRITC-DHPE at a weight ratio of 19:1. A microplate reader (CLARIO star, BMG Labtech, Ortenberg, Germany) was used to measure fluorescence intensity.

2.4. Preparation of HCP-DOTAP MCLVs

HCPs were dialyzed to remove salts using an MWCO 100 – 500 Da dialysis tubing (Spectrum Laboratories Inc., Rancho Dominguez, CA, USA) at 4 ˚C for 7 days. MCLVs were prepared by mixing 500 μL of HCP with 500 μL of DOTAP and incubated at room temperature for 10 min.

2.5. Encapsulation efficiency of HCP in MCLVs

Free HCPs were collected from MCLVs by ultracentrifugation to calculate the encapsulation efficiency of HCPs within MCLVs. Ultracentrifugation was performed at 84,000 rpm (193,617 rcf) at 4 ˚C for 2 h (Optima TLX Ultracentrifuge 120,000, Beckman, Pasadena, CA, USA). The concentration of free HCPs was measured using the micro-BCA protein assay kit (Pierce Biotechnology, Rockford, IL, USA).

2.6. Cryogenic transmission electron microscopy (Cryo-TEM)

Cryo-TEM specimens were prepared with a thin film of aqueous solution (3 – 9 μL) of the prepared lipid vesicles on a lacey-supported grid (Quantifoil R 1.2/1.3 300 mesh, Copper, Electron Microscopy Sciences, Hatfield, PA, USA) by the plunge-dipping method. The thin aqueous films were rapidly vitrified by plunging them into liquid ethane after blotting the excess liquid on the grid with a filter paper for 2 – 3 sec. Cryo-TEM images were collected using JEM-3011 HR (JEOL Ltd., Tokyo, Japan) equipped with a Gatan 626 cryo-holder (Gatan

Inc., Pleasanton, CA, USA) under 300 kV. The data were analyzed with Gatan Digital Micrograph software (Gatan Inc., Pleasanton, CA, USA).

2.7. Small angle X-ray scattering (SAXS)

SAXS analysis was performed at the 4C SAXS II beamline at the Pohang Accelerator Laboratory (Pohang, Republic of Korea) [18,19]. The lipid particles were detected under 0.734 of X-ray beam wavelength with 2 m of sample-to-detector distance (SDD) for 10 sec at 25 °C. The magnitude of the scattering vector ($q = (4\pi/\lambda)sin\theta$, θ = scattering angle) was determined between 0.01 $Å^{-1}$ and 0.3 $Å^{-1}$. Polyethylene-*b*-polybutadiene-*b*-polystyrene (SEBS) block copolymer was used as a calibration standard. The interlamellar distance was measured by the SAXS correlation equation of $2\pi/q$. The solution samples were investigated with a quartz capillary (outside diameter = 1.5 mm and wall thickness = 0.01 mm).

3. Results and Discussion

3.1. HCP-induced self-assembly of LUVs into MCLVs

The prepared DOTAP LUVs had a mean diameter and zeta potential of 161 ± 2.6 nm and 52.9 ± 0.6 mV, respectively, as determined by DLS. HCP used in this work had a molecular weight of ~ 1.57 kDa according to MALDI-TOF analysis (Fig. S1, Supporting Information). HCP was dialyzed against deionized water to remove residual salts. Dialysis did not affect the random coil structure of HCP (Fig. S2 and Table S1). The pre-formed DOTAP LUVs were simply mixed with HCPs at a 1:1 volumetric ratio at 25 °C for 10 min to generate MCLVs (**Fig. 2a**). The encapsulation efficiencies of HCPs into MCLVs were 83.3 ± 1.4 and 80.0 ± 2.5 % at WR = 2 and 3, respectively, at 50 mM sodium chloride (pH 7.4) even though the target loading yield was very high, ~ 55.5 %. The size distribution and zeta potential were determined at various weight ratios (WRs) of HCP to DOTAP (**Fig. 2b**). The hydrodynamic diameter of the resulting MCLVs was 156.7 ± 0.9 nm at WR = 2.0, slightly smaller than that of DOTAP LUVs (161 ± 2.6 nm). The charge neutralization was also observed as the zeta potential dramatically decreased from 52.9 ± 0.6 mV to 17.9 ± 1.4 mV (WR = 5.0) as LUVs were complexed with HCPs. The decreased zeta potential and particle size of MCLVs suggest the facile binding of HCPs onto the surface of DOTAP LUVs, resulting in significant morphological changes of LUVs during the formation of multilamellar structures as observed in the DNA-lipid and globular protein-lipid complexation [18,19]. Note that the simple coating of LUVs with HCPs cannot explain the shrinkage of LUVs.

CNP, a key component for skin barrier function, was incorporated into the lipid vesicles to further enhance the robustness of lipid membranes. The length asymmetry of the two alkyl chains in CNP helps to maintain the interaction between the inner leaflet and the outer leaflet of the lipid membrane [29]. The mean diameter and zeta potential of LUVs and MCLVs (WR = 2 and 3) were determined at various weight percentages of CNP (**Fig. 2c and 2d**). Although no clear correlation was observed between the weight percentage of CNP and colloidal properties, the addition of CNP to LUVs increased their mean diameter and zeta potential. In particular, the diameter and zeta potential of LUVs significantly increased when 5 wt% CNP was incorporated, indicating the increased lateral packing of lipids in the lamellar structure of LUVs. Despite the largest LUVs at 5 wt% CNP, their complexation with HCP resulted in the smallest HCP-DOTAP/CNP MCLVs presumably due to the strong electrostatic

interaction.

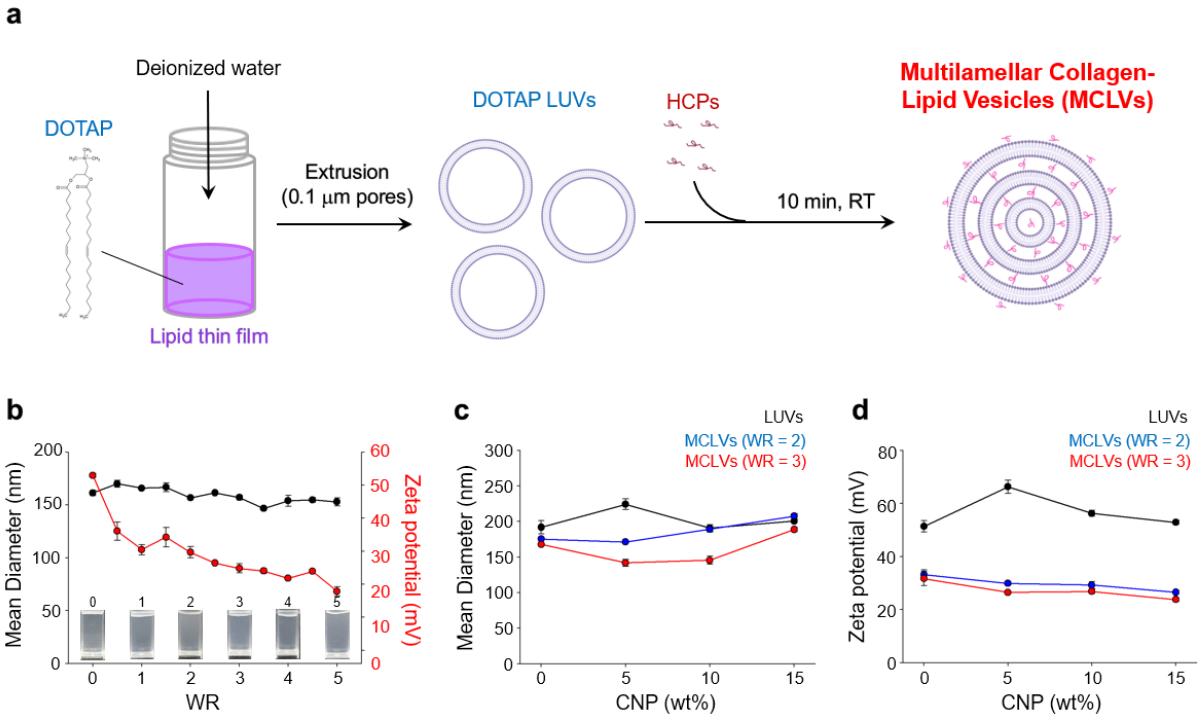

Fig. 2. Preparation and characterization of HCP-DOTAP MCLVs. (a) Schematic illustration of the preparation procedures of MCLVs. (b) Hydrodynamic size and zeta potential of MCLVs at various WRs (black = mean diameter and red = zeta potential). (c) The hydrodynamic size at various weight percentages of CNP (black = LUVs, red = MCLVs at WR = 2, and blue = MCLVs at WR = 3). (d) Zeta potential at various weight percentages of CNP (black = LUVs, red = MCLVs at WR = 2, and blue = MCLVs at WR = 3).

3.2. HCP-mediated morphological changes of LUVs to MCLVs

Cryo-TEM analysis was carried out to investigate the morphological evolution of DOTAP LUVs and DOTAP/CNP LUVs (5 wt% CNP) to HCP-DOTAP MCLVs and HCP-DOTAP/CNP MCLVs. The prepared MCLVs exhibited multilamellar structures with different numbers of layers and inter-layer distances, while LUVs had a unilamellar structure (**Fig. 3a-d** and Fig. S3). The lipid membrane thickness increased from LUVs to MCLVs due to the binding of HCPs to the surface of vesicles. Furthermore, the interaction led to the molecular rearrangement of the hybridized HCP-lipid structure to MCLVs [18]. Cryo-TEM images of MCLVs exhibit multiple intermediate structures, including folded vesicles and partially fused vesicles (Fig. S3, Supporting Information). Some wrapped LUVs exhibited folded and collapsed structures. Besides, MCLVs with a higher number of lamellar layers were observed when CNP was added. In the presence of 5 wt% CNP, the self-assembly of LUVs into MCLVs appears to be more efficient through the stronger electrostatic attraction with HCPs due to the increased zeta potential of LUVs as shown in Fig. 2d.

The SAXS analysis of HCP-DOTAP MCLVs and HCP-DOTAP/CNP MCLVs exhibited a typical SAXS profile for multilamellar structures with a pronounced peak position ratio of 1:2:3 (**Fig. 3e** and Fig. S4). The measured interlayer distance ($d_{lamellar}$) was ~ 11.4 nm, while LUVs had a $d_{lamellar}$ of ~ 9.0 nm, which was the simple sum of the thicknesses of two lipid membranes. The value seems to originate from aggregated LUVs at the high concentration ($\geq$ 2 mg mL^{-1}) as concentrated samples were used for SAXS analysis. As the hybrid membrane thickness was 6.8 ± 2.3 nm as estimated from cryo-TEM images, the calculated distance of the interstitial aqueous space was ~ 4.6 nm, a reasonable distance between the lipid bilayers in which HCPs to be trapped. The self-assembly of HCPs with DOTAP/CNP LUVs also exhibited a similar $d_{lamellar}$ (**Fig. 3f**) as CNPs affect the lateral ordering of lipid molecules rather than the bilayer thickness [30].

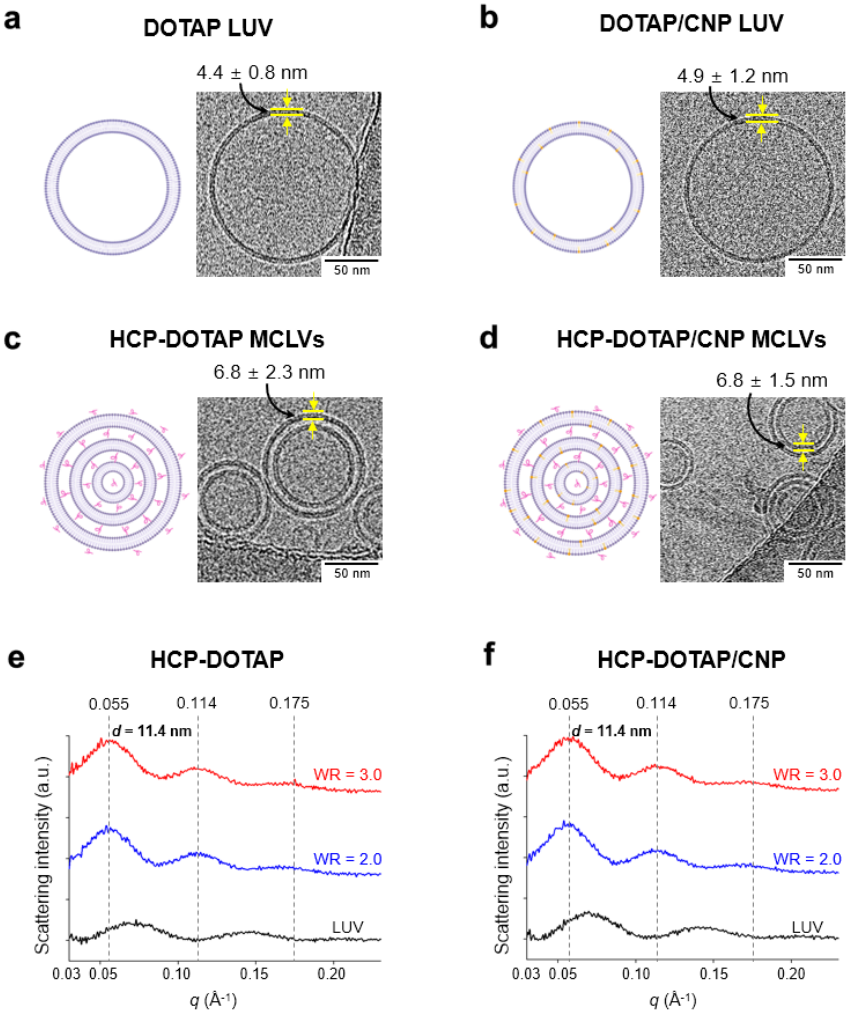

Fig. 3. Structural analysis of HCP-DOTAP MCLVs. Cryo-TEM images of DOTAP LUVs (a), DOTAP/CNP LUVs (b), HCP-DOTAP MCLVs (c), and HCP-DOTAP/CNP MCLVs (d). SAXS profiles of HCP-DOTAP LUVs (e) and HCP-DOTAP/CNP MCLVs (f).

Furthermore, we investigated the multilamellar self-assembly of LUVs with HCPs using FRET analysis. LUVs incorporating FRET donors and acceptors were prepared by dissolving the lipids with fluorescein-DHPE (denoted 'f-DOTAP', λ_{ex} = 496 nm and λ_{em} = 519 nm) and TRITC-PE (denoted 't-DOTAP', λ_{ex} = 544 nm and λ_{em} = 570 nm), respectively, at a weight ratio of 19:1 (**Fig. 4a**). f-DOTAP and t-DOTAP were prepared separately and then mixed together with HCP to induce the vesicle-to-vesicle self-assembly, which led to FRET between the vesicles with efficiencies of 8.6 ± 0.8 % and 5.1 ± 0.9 % for HCP-DOTAP and HCP-DOTAP/CNP, respectively (**Fig. 4b-e**). Therefore, all of the findings in cryo-TEM, SAXS, and FRET analyses suggest that the HCP-mediated attractive interactions between LUVs can induce the formation of multilayered hybrid structures.

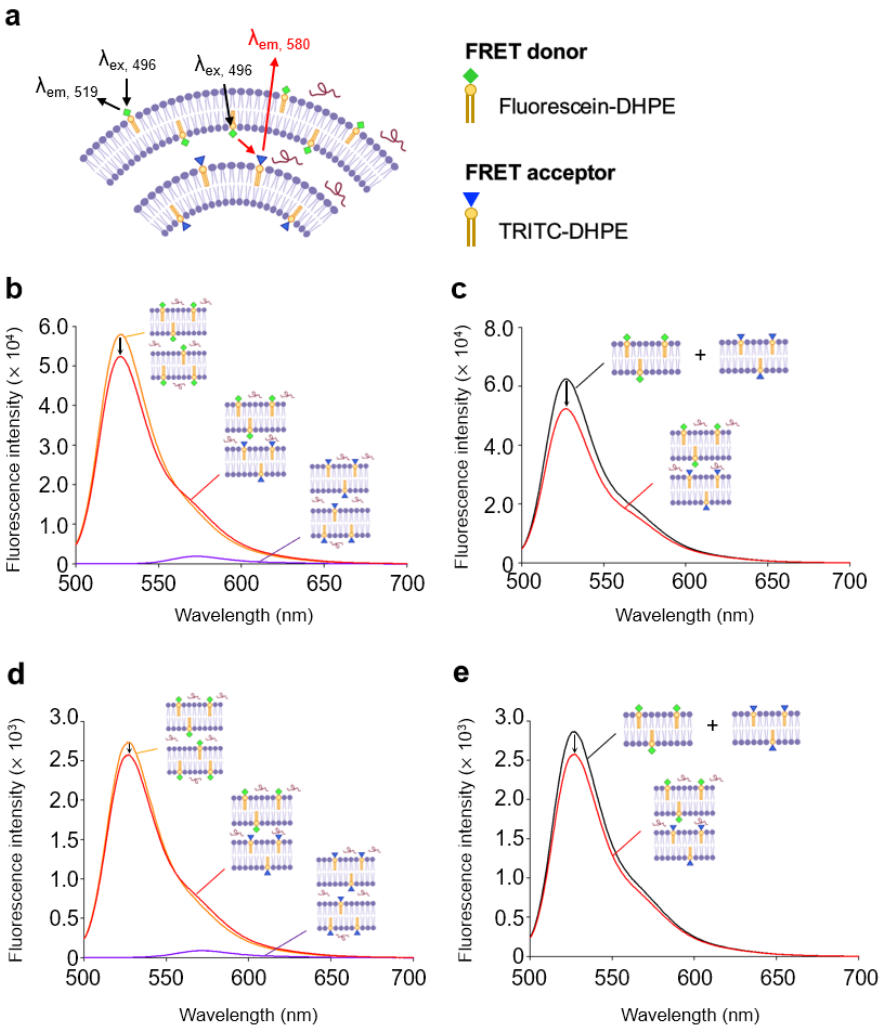

Fig. 4. Self-assembly into MCLVs. (a) Schematic illustration of FRET analysis. Fluorescence profiles of HCP-DOTAP MCLVs (b and c) and HCP-DOTAP/CNP MCLVs (d and e).

3.3. Structural stability of HCP-DOTAP MCLVs

Next, we investigated the effects of multilamellar self-assembly on the structural stability of lipid vesicles. Firstly, the long-term dispersion stability of LUVs and MCLVs (WR = 2 and 3) was examined in 50 mM sodium chloride at various temperatures: 4, 25, 37, and 45 °C (**Fig. 5a-d**). The addition of CNPs did not significantly affect the initial hydrodynamic size of LUVs, though the temporal variation of DOTAP/CNP LUVs became clearly lower than that of DOTAP LUVs (**Fig. 5e** and S5). The reduction of size variation by CNPs was less evident for MCLVs; however, HCP-DOTAP/CNP MCLVs still exhibited excellent dispersion stability at WR = 3.5 while HCP-DOTAP MCLVs showed structural instability (e.g., aggregation) after 10-day incubation (**Fig. 5f-h**). As for the surface charge density inferred from zeta potential measurements, both of DOTAP and DOTAP/CNP LUVs maintained similar values around 60 mV regardless of the incubation temperatures (Fig. S6 and S7). However, as WR increased (more HCPs were added), zeta potential decreased because negatively charged HCPs bind to and electrostatically screen the surface of lipid vesicles (Fig. S6). Interestingly, large variations were observed for HCP-DOTAP MCLVs. In particular, the zeta potential of HCP-DOTAP MCLVs was smaller than 10 mV at WR = 3.5, which can induce colloidal instability due to reduced double-layer forces. In contrast, HCP-DOTAP/CNP MCLVs still exhibited zeta potential values around 20 mV at all of the temperatures tested (Fig. S7). The results support the higher structural stability of HCP-DOTAP/CNP MCLVs, indicating the contribution of CNPs to the stabilization of lipid bilayer integrity.

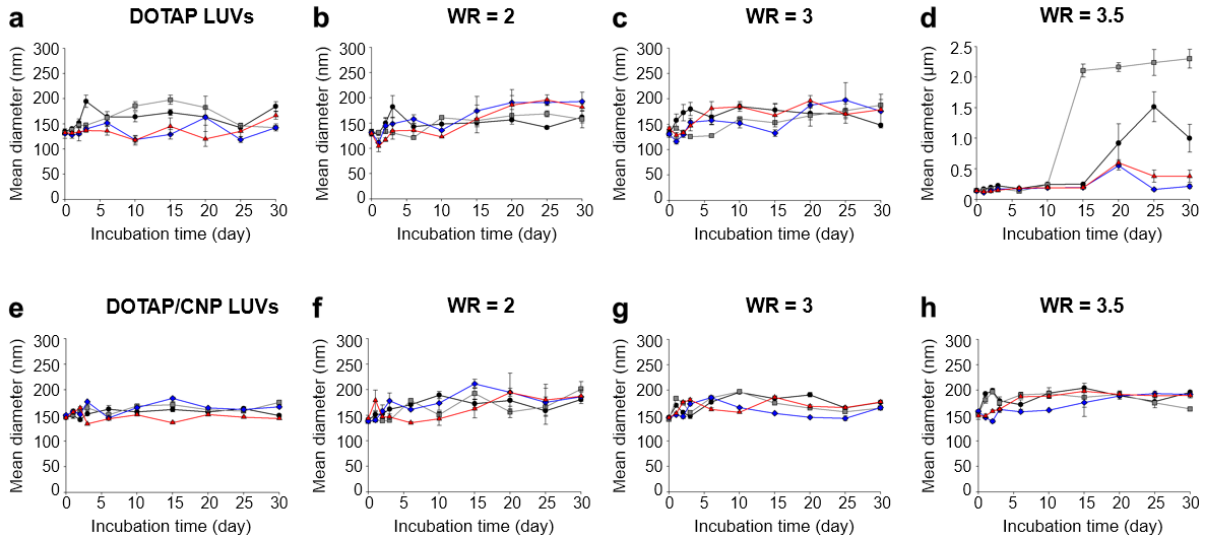

Fig. 5. Dispersion stability of lipid vesicles. Dispersion stability of DOTAP LUVs (a), HCP-DOTAP MCLVs at WR = 2 (b), 3 (c), and 3.5 (d), DOTAP/CNP LUVs (e), HCP-DOTAP/CNP MCLVs at WR = 2 (f), 3 (g), and 3.5 (h) at various temperatures: black, 4 °C; gray, 25 °C; blue, 37 °C; and red, 45 °C.

Secondly, we examined the structural stability of MCLVs against chemical stresses, such as surfactants and salts. The hydrodynamic size changes of LUVs and MCLVs were determined in the presence of sodium dodecyl sulfate (SDS) at room temperature for 3 h (Fig. S8a). SDS is a detergent that can efficiently dissolve lipids in the membrane and solubilize

them in an aqueous solution at a concentration above critical micelle concentration (c.m.c.), 8 mM corresponding to ~ 0.2 wt% [31]. LUVs and MCLVs were treated with SDS at two different concentrations, 0.125 wt% and 0.25 wt%, to examine its disturbing effect on the lipid membrane integrity. As expected, the hydrodynamic size of DOTAP LUVs markedly decreased at both concentrations. However, DOTAP/CNP LUVs maintained their size at 0.125 wt%, indicating the stabilization effect of CNP presumably due to the increased lateral packing [30]. In contrast to LUVs, all of MCLVs maintained their original size under the same condition, which indicates that the layer-by-layer self-assembly supports the outermost layer and prevents the surfactant-induced lipid dissociation. Also, the dispersion stability of lipid vesicles was examined at 0 – 1000 mM NaCl for 10 h (Fig. S8b). While DOTAP LUVs and HCP-DOTAP MCLVs (WR = 2) exhibited relatively larger variations, DOTAP/CNP LUVs and HCP-DOTAP/CNP MCLVs (WR = 2) maintained their original hydrodynamic size even at high NaCl concentrations due to the stabilization effect of CNP.

Finally, the dispersion stability of LUVs and MCLVs was examined under repeated freeze/thaw cycles and freeze-drying, which are very harsh conditions for colloids [32]. The mean diameter of the lipid vesicles was measured during 5 repetitions of freezing and thawing for 10 h and 5 h, respectively (**Fig. 7a**). While DOTAP LUVs exhibited a dramatic increase in hydrodynamic size even after the first cycle, DOTAP/CNP LUVs and all MCLVs maintained sub-micron sizes and were still well-dispersed up to four cycles. In particular, HCP-DOTAP/CNP MCLVs at WR = 2 exhibited excellent structural stability without significant size changes, indicating the superior robustness of the multilamellar structure reinforced by HCP-mediated layer-by-layer self-assembly and ceramide-enhanced lipid ordering. All of the samples tested showed a large increase in size after five cycles, possibly implying that molecular disorganization might undergo during repeated freeze/thaw processes though the apparent size changes were not observed. The results are supported by cryo-TEM analysis as multilamellar structures were clearly observed in HCP-DOTAP/CNP MCLVs after the third cycle of freeze-thaw processes, while DOTAP LUVs were severely aggregated after the first cycle (Fig. S9). HCP-DOTAP/CNP MCLVs prepared using a higher amount of HCP (WR = 3) showed larger size changes, which indicates that the ratio of HCP to LUVs needs to be minimized to generate stable MCLVs as also shown in Fig. 5. The exposure of LUVs and MCLVs to freeze-drying conditions also indicates the excellent structural stability of MCLVs (**Fig. 7b**). Both LUVs were aggregated to form much larger particles, while the mean diameter of MCLVs increased to about 250 nm except HCP-DOTAP/CNP MCLVs at WR = 3. Despite the differences in size, no significant changes in zeta potential values of the lipid vesicles by freeze-drying were observed, indicating that the size changes were mechanically driven to form larger aggregates while maintaining the surface structures of lipid vesicles (Fig. S10).

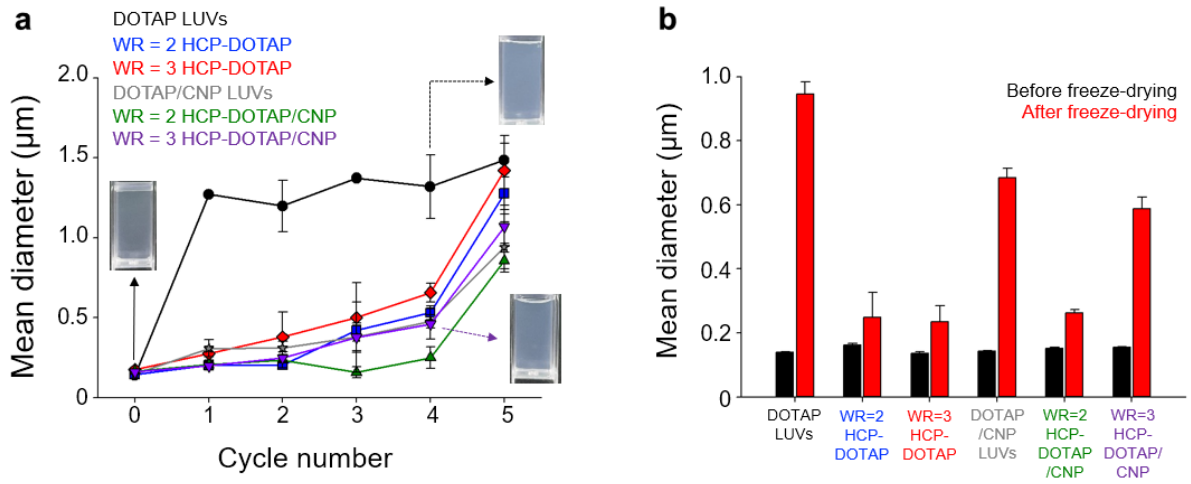

Fig. 7. Improved dispersion stability of MCLVs under harsh conditions. The hydrodynamic size changes of lipid vesicles during freeze-thaw cycles (a) and after freeze-drying (b).

4. Conclusions

In summary, we demonstrated that protein-induced vesicle-to-vesicle self-assembly can make highly robust multilamellar hybrid structures. HCP-induced multilamellar structures were fabricated by simply mixing HCP with pre-formed LUVs under ambient conditions. No high-power instruments and organic solvents were used. HCP-DOTAP MCLVs had an encapsulation efficiency of > 80 % at 50 mM NaCl and long-term dispersion stability. Cryo-TEM and SAXS analyses revealed the morphological evolution of LUVs into multilamellar structures. FRET assays also showed that HCP was very densely embedded between the lipid multilayers, reflecting the high encapsulation efficiency and stabilization effects. Besides, CNP enhanced the dispersion stability of MCLVs by improving the robustness of the lipid membranes even under very harsh conditions, such as repeated freeze-thaw stresses. Our findings suggest that the self-assembly of proteins and pre-formed lipid vesicles is a very simple and promising approach to the efficient stabilization of lipid vesicles.

Acknowledgments

This work was financially supported by Cosmax, Inc (Seongnam, Republic of Korea). This research was also supported by a grant of the Korea Health Technology R&D Project through the Korea Health Industry Development Institute (KHIDI), funded by the Ministry of Health & Welfare, Republic of Korea (HV22C0209). Experiments at PLS-II were supported in part by MSIP and POSTECH.

Appendix A. Supplementary data

Supplementary data to this article can be found online at https://doi.org/XXXXXX.

Author Information

ORCID

Bon Il Koo: 0000-0003-3695-7579
Rafia Tasnim Rahman: 0000-0002-0477-2871
Dong Jae Lee: 0000-0003-2041-9979
Yoon Sung Nam: 0000-0002-7302-6928

References

[1] C. Sinico, A.M. Fadda, Vesicular carriers for dermal drug delivery, Exp. Opin. Drug Deliv. 6 (8) (2009) 813-825, https://doi.org/10.1517/17425240903071029.

[2] J. Swaminathan, C. Ehrhardt, Liposomal delivery of proteins and peptides, Exp. Opin. Drug Deliv. 9 (12) (2012) 1489-1503, https://doi.org/10.1517/17425247.2012.735658.

[3] C. Kataoka-Hamai, H. Inoue, Y. Miyahara, Detection of supported lipid bilayers using their electric charge, Langmuir 24 (17) (2008) 9916-9920, https://doi.org/10.1021/la801623m.

[4] Y.S. Nam, J.W. Kim, J. Park, J. Shim, J.S. Lee, S.H. Han, Tocopheryl acetate nanoemulsions stabilized with lipid-polymer hybrid emulsifiers for effective skin delivery, Colloids and Surfaces B: Biointerfaces 94 (2012) 51-57,

[5] S.J. Shepherd, D. Issadore, M.J. Mitchell, Microfluidic formulation of nanoparticles for biomedical applications, Biomaterials 274 (2021) 120826, https://doi.org/10.1016/j.biomaterials.2021.120826.

[6] S.L. Regen, B. Czech, A. Singh, Polymerized vesicles, J. Am. Chem. Soc. 102 (21) (1980) 6638–6640, https://doi.org/10.1021/ja00541a078.

[7] I. Stanish, J. P. Santos, A. Singh, One-step, chemisorbed immobilization of highly stable, polydiacetylenic phospholipid vesicles onto gold films, J. Am. Chem. Soc. 123 (5) (2001) 1008–1009, https://doi.org/10.1021/ja0056623.

[8] S. Liu, D. O'Brien, Stable polymeric nanoballons: lyophilization and rehydration of cross-linked liposomes, J. Am. Chem. Soc. 124 (21) (2002) 6037–6042, https://doi.org/10.1021/ja0123507.

[9] J. Hotz, W. Meier, Vesicle-templated polymer hollow spheres, Langmuir 14 (5) (1998) 1031–1036, https://doi.org/10.1021/la971080w.

[10] D.D. Lasic, Sterically stabilized vesicles, Angew. Chem. Int. Ed. Engl. 33 (17) (1994) 1685–1698, https://doi.org/10.1002/anie.199416851.

[11] V.D. Leo, F. Milano, Recent advancements in polymer/liposome assembly for drug delivery: from surface modifications to hybrid vesicles, Polymers 13 (7) (2021) 1027, https://doi.org/10.3390/polym13071027.

[12] J.J. Moon, H. Suh, A. Bershteyn, M.T. Stephan, H. Liu, B. Huang, M. Sohail, S. Luo, S.H. Um, H. Khant, J.T. Goodwin, J. Ramos, W. Chiu, D.J. Irvine, Interbilayer-crosslinked

multilamellar vesicles as synthetic vaccines for potent humoral and cellular immune responses, Nat. Mater. 10 (3) (2011) 243-251, https://doi.org/10.1038/nmat2960.

[13] J.J. Moon, H. Suh, A.V. Li, C.F. Ockenhouse, A. Yadava, D.J. Irvine, Enhancing humoral responses to a malaria antigen with nanoparticle vaccines that expand Tfh cells and promote germinal center induction, Proc. Natl. Acad. Sci. 109 (4) (2012) 1080-1085, https://doi.org/10.1073/pnas.1112648109.

[14] Y. Fan, S.M. Stronsky, Y. Xu, J.T. Steffens, S.A. Tongeren, A. Erwin, C.L. Cooper, J.J. Moon, Multilamellar vaccine particle elicits potent immune activation with protein antigens and protects mice against Ebola virus infection, ACS Nano 13 (10) (2019) 11087-11096, https://doi.org/10.1021/acsnano.9b03660.

[15] Y. Cao, X. Dong, X. Chen, Polymer-modified liposomes for drug delivery: from fundamentals to applications, Pharmaceutics 14 (4) (2022) 778, https://doi.org/10.3390/pharmaceutics14040778.

[16] S.-M. Lee, H. Chen, C.M. Dettmer, T.V. O'Halloran, S.T. Nguyen, Polymer-caged liposomes: a pH-responsive delivery system with high stability, J. Am. Chem. Soc. 129 (49) (2007) 15096-15097, https://doi.org/10.1021/ja070748i.

[17] J.-H. Park, H.-J. Cho, H.Y. Yoon, I.-S. Yoon, S.-H. Ko, J.-S. Shim, J.-H. Cho, J.-H. Park, K. Kim, I.C. Kwon, D.-D. Kim, Hyaluronic acid derivative-coated nanohybrid liposomes for cancer imaging and drug delivery, J. Cont. Rel. 174 (2014) 98-108. https://doi.org/10.1016/j.jconrel.2013.11.016.

[18] B.I. Koo, I. Kim, M.Y. Yang, S.D. Jo, K. Koo, S.Y. Shin, K.M. Park, J.M. Yuk, E. Lee, Y.S. Nam, Protein-induced metamorphosis of unilamellar lipid vesicles to multilamellar hybrid vesicles, J. Control. Rel. 331 (2021) 187-197, https://doi.org/10.1016/j.jconrel.2021.01.004.

[19] B.I. Koo, S.M. Jin, H. Kim, D.J. Lee, E. Lee, Y.S. Nam, Conjugation-free Multilamellar Protein-lipid Hybrid Vesicles for Multifaceted Immune Responses, Adv. Healthcare Mater. 10 (22) (2021), 2101239, https://doi.org/10.1002/adhm.202101239.

[20] J.O. Radler, I. Koltover, T. Salditt, C.R. Safinya, Structure of DNA-cationic liposome complexes: DNA intercalation in multilamellar membranes in distinct interhelical packing regimes, Science 275 (5301) (1997) 810-814, https://doi.org/10.1126/science.275.5301.810.

[21] N.F. Bouxsein, C. Leal, C.S. McAllister, K.K. Ewert, Y.L. Li, C.E. Samuel, C.R. Safinya, Two-dimensional packing of short DNA with nonpairing overhangs in cationic liposome-DNA complexes: from onsager nematics to columnar nematics with finite-length columns, J. Am. Chem. Soc. 133 (19) (2011) 7585-7595, https://doi.org/10.1021/ja202082c.

[22] S.D. Jo, J.S. Kim, I. Kim, J.S. Yun, J.C. Park, B.I. Koo, E. Lee, Y.S. Nam, DNA lipoplex-based light-harvesting antennae, Adv. Funct. Mater. 27 (26) (2017) 1700212, https://doi.org/10.1002/adfm.201700212.

[23] G. Subramanian, R.P. Hjelm, T.J. Deming, G.S. Smith, Y. Li, C.R. Safinya, Structure of

complexes of cationic lipids and poly(glutamic acid) polypeptides: a pinched lamellar phase, J. Am. Chem. Soc. 122 (1) (2000) 26-34, https://doi.org/10.1021/ja991905j.

[24] L.H. Yang, H.J. Liang, T.E. Angelini, J. Butler, R. Coridan, J.X. Tang, G.C.L. Wong, Self-assembled virus-membrane complexes, Nat. Mater. 3 (9) (2004) 615-619, https://doi.org/10.1038/nmat1195.

[25] E. Henry, A. Dif, M. Schmutz, L. Legoff, F. Amblard, V. Marchi-Artzner, F. Artzner, Crystallization of fluorescent quantum dots within a three-dimensional bio-organic template of actin filaments and lipid membranes, Nano Lett. 11 (12) (2011) 5443-5448, https://doi.org/10.1021/nl203216q.

[26] León-López A, Morales-Peñaloza A, Martínez-Juárez VM, Vargas-Torres A, Zeugolis DI, Aguirre-Álvarez G. Hydrolyzed Collagen-Sources and Applications. Molecules 24 (22) (2019) 4031, doi: 10.3390/molecules24224031.

[27] U. Bulbake, S. Doppalapudi, N. Kommineni, W. Khan, Liposomal formulations in clinical use: an updated review, Pharmaceutics 9 (2) (2017) 12, https://doi.org/10.3390/pharmaceutics9020012.

[28] U. Yokose, J. Ishikawa, Y. Morokuma, A. Naoe, Y. Inoue, Y. Yasuda, H. Tsujimura, T. Fujimura, T. Murase, A. Hatamochi, The ceramide [NP]/[NS] ratio in the stratum corneum is a potential marker for skin properties and epidermal differentiation, BMC Dermatology 20 (1) (2020) 1-20, https://doi.org/10.1186/s12895-020-00102-1.

[29] T.N. Engelbrecht, A. Schroeter, T. Hauβ, B. Demé, H.A. Scheidt, D. Huster, R.H.H. Neubert, The impact of ceramides NP and AP on the nanostructure of *stratum corneum* lipid bilayer. Part I: neutron diffraction and ^{2}H NMR studies on multilamellar models based on ceramides with symmetric alkyl chain length distribution, Soft Matter 8 (24) (2012) 6599-6607. https://doi.org/10.1039/C2SM25420D.

[30] T. Schmitt, S. Lange, B. Dobner, S. Sonnenberger, T. Haub, R. H. H. Neubert, Investigation of a CER[NP]- and [AP]-based stratum corneum modeling membrane system: using specifically deuterated CER together with a neutron diffraction approach, Langmuir 34 (4) (2018) 1742-1749. https://doi.org/10.1021/acs.langmuir.7b01848.

[31] S.A. Markarian, L.R. Harutyunyan, R.S. Harutyunyan, The properties of mixtures of sodium dodecylsulfate and diethylsulfoxide in water, Journal of Solution Chemistry 34 (3) (2005) 361-368. https://doi.org/10.1007/s10953-005-3056-x.

[32] T.H.L. Kim, H. Jun, Y.S. Nam, Importance of crystallinity of anchoring block of semi-solid amphiphilic triblock copolymers in stabilization of silicon nanoemulsions, Journal of Colloid and Interface Science 503 (2017) 39-46. https://doi.org/10.1016/j.jcis.2017.04.079.